Chinese Chemical Letters 37 (2026) 111642

Contents lists available at ScienceDirect

Chinese Chemical Letters

journal homepage: www.elsevier.com/locate/cclet

Development of Globo-H conjugated bacteriophage Qβ mutant virus-like particles as an anticancer vaccine

Yuanzhan Wang, Qingyu Zhao, Xuanjun Wu*

National Glycoengineering Research Center, Shandong Key Laboratory of Carbohydrate Chemistry and Glycobiology, NMPA Key Laboratory for Quality Research and Evaluation of Carbohydrate-based Medicine, Shandong Key Laboratory of Carbohydrate and Carbohydrate-conjugate Drugs, Shandong University, Qingdao 266237, China

ARTICLE INFO

Article history:
Received 24 May 2025
Revised 23 July 2025
Accepted 25 July 2025
Available online 26 July 2025

Keywords:
Tumor-associated carbohydrate antigen (TACA)
Globo-H
Bacteriophage Qβ
Cancer
Vaccine

ABSTRACT

Globo-H is a tumor-associated carbohydrate antigen (TACA) that is overexpressed in various cancers, making it a promising target for anticancer vaccine development. However, traditional conjugate vaccines, such as those linked to keyhole limpet hemocyanin (KLH) or cross-reactive material 197 (CRM197), have demonstrated limited clinical efficacy. To address this limitation, we developed an innovative vaccine candidate by conjugating chemoenzymatically synthesized Globo-H to a mutant of bacteriophage Qβ (mQβ) virus-like particle. The resulting mQβ-Globo-H conjugate elicited significantly higher levels of anti-Globo-H IgG antibodies in mice compared to both KLH-Globo-H and CRM197-Globo-H conjugates. Furthermore, the antibodies produced by the mQβ-Globo-H conjugate exhibited strong binding to MCF-7 breast cancer cells and triggered potent complement-dependent cytotoxicity (CDC) against these cancer cells. In contrast, negligible antibody binding and CDC effects were observed against normal MCF-10A breast epithelial cells. This new conjugate vaccine also produced robust humoral responses in rabbits, with the resulting antibodies exhibiting high selectivity for human breast cancer tissues. These findings underscore the clinical translational potential of the mQβ-Globo-H conjugate vaccine.

© 2026 Published by Elsevier B.V. on behalf of Chinese Chemical Society and Institute of Materia Medica, Chinese Academy of Medical Sciences.

Carbohydrate-based vaccines offer a promising approach for cancer treatment [1–3]. A key component of these vaccines is tumor-associated carbohydrate antigens (TACAs), which include Thomsen-nouveau (Tn), Thomsen-Friedenreich (Tf), sialyl-Tn (sTn), Globo-H, stage-specific embryonic antigen (SSEA)-4, SSEA-3, GM2, GD2, GD3, sialyl Lewis^X (sLe^X), and sialyl Lewis^a (sLe^a) [4]. Among these, Globo-H stands out as a promising target for anticancer vaccine development because it is overexpressed on the surface of various cancer cells, including those in breast, lung, gastric, pancreatic, ovarian, and prostate cancers [5]. However, one major challenge in vaccine development is the low inherent immunogenicity of Globo-H. To address this issue, Globo-H has been conjugated with keyhole limpet hemocyanin (KLH), resulting in the KLH-Globo-H conjugate [6]. In the phase I clinical trial of KLH-Globo-H plus QS-21 involving 27 metastatic breast cancer patients, 16 patients produced IgM antibodies that effectively bound to MCF-7 cells, though IgG reactivity was limited [7]. In the phase II trial (348 patients), adagloxad simolenin (AS, KLH-Globo-H) plus OBI-821 was administered to 224 patients, inducing anti-Globo-H IgM in 199 patients and IgG in 182 patients [8]. Although the combination of AS and OBI-821 did not lead to an improvement in progression-free survival (PFS), patients with high titers of anti-Globo-H IgG exhibited longer PFS compared to those with lower levels. Currently, a phase III clinical trial of AS/OBI-821 is underway for patients with triple-negative breast cancer (NCT03562637) [9].

Given the significant promise of the Globo-H antigen, researchers are exploring new Globo-H vaccine candidates [10–16]. Wong and co-workers developed a conjugate of diphtheria toxoid cross-reactive material 197 (CRM197) with Globo-H, resulting in anti-Globo-H IgG antibodies that are comparable to those generated by the KLH-Globo-H conjugate [10]. They further optimized the immunogen by azide-modifying Globo-H at the C-6 position on either fucose or galactose (Gal). The modified Globo-H was chemically linked to CRM197 and adjuvanted with C34 to enhance immunogenicity [11,12]. Ye and co-workers reported a conjugate of CRM197 with fluorinated *N*-acyl Globo-H, also using C34 to boost immune response [13]. Li and co-workers demonstrated that the CRM197-Globo-H conjugate, when paired with QS-21 and 3D-MPL adjuvants, induced potent IgG2a and IgG3 antibodies; these antibodies showed improved binding to MCF-7 cells, as well as enhanced complement-dependent cytotoxicity

* Corresponding author.
E-mail address: xuanjun@sdu.edu.cn (X. Wu).

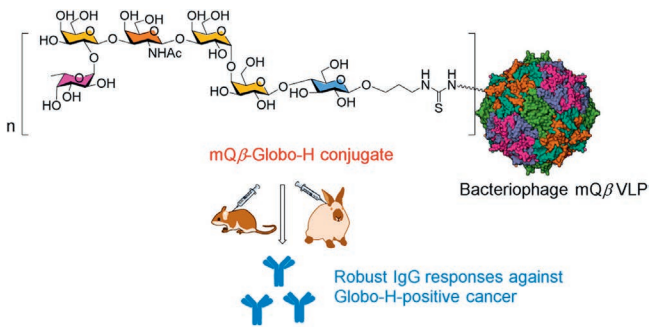
https://doi.org/10.1016/j.cclet.2025.111642
1001-8417/© 2026 Published by Elsevier B.V. on behalf of Chinese Chemical Society and Institute of Materia Medica, Chinese Academy of Medical Sciences.

(CDC) and antibody-mediated cellular phagocytosis [14]. Additionally, Guo and co-workers developed a monophosphoryl lipid A (MPLA)-Globo-H conjugate that generated strong IgG antibodies specifically targeting Globo-H-positive MCF-7 cells [15].

Despite extensive efforts to enhance the immunogenicity of Globo-H (or modified Globo-H) through conjugation with KLH [6–8], CRM197 [10–14], or MPLA [15], current clinical evidence indicates that the existing Globo-H-based vaccine candidates show limited potential for achieving clinical efficacy. A likely reason for this is that the quality and quantity of antibodies induced by current vaccine candidates are insufficient to provide tumor protection for the entire patient population. Consequently, novel approaches to Globo-H conjugate design are urgently needed to ensure clinical success.

Unlike amorphous carriers such as KLH, bacteriophage Qβ virus-like particles (VLPs) have well-defined three-dimensional structures that allow for high-density and organized antigen presentation, which is crucial for effective antibody production [17]. Furthermore, Qβ VLPs can encapsulate RNA, activating Toll-like receptor 7 and enhancing the immunogenicity of the conjugate even further [18]. Over the past decade, Huang and co-workers have explored the use of wild-type bacteriophage Qβ VLPs to develop various Qβ-TACA conjugates, including Qβ-Tn [19,20], Qβ-GM2 [21], Qβ-MUC1-Tn [22], and Q$\beta-$9NHAc-GD2 [23]. While Qβ-TACA can induce potent TACA-specific antibodies, it also leads to the production of high levels of carrier-specific antibodies. To address this issue, Huang and co-workers developed a triple mutant of bacteriophage Qβ (mQβ), which features the A38K, A40C, and D102C mutations [24]. The mQβ platform presents several key advantages for vaccine development. First, the A38K mutation eliminates potential B-cell epitopes on Qβ while introducing a lysine residue for efficient TACA conjugation, thereby further shielding adjacent B-cell epitopes on the coat protein. This modification minimizes immune responses against the carrier itself. Second, the A40C and D102C mutations create cross-subunit disulfide bonds, enhancing thermal stability and prolonging the construct's *in vivo* half-life. Third, compared to Qβ-TACA, mQβ-TACA elicits stronger TACA-specific antibody responses while markedly reducing anticarrier antibody production. Together, these features underscore mQβ's strong potential as a versatile vaccine platform.

The mQβ platform has demonstrated efficacy as a versatile carrier for diverse antigens, including TACA (Tn, or sLe^a) [24,25], the heroin mimicking small-molecule hapten 6-AmHap [26], the receptor binding domain (RBD) of the SARS-CoV-2 spike protein [27], and poly-β-(1–6)-*N*-acetylglucosamine (PNAG) [28]. However, mQβ has not yet been investigated for use in a Globo-H conjugate vaccine. In this study, we developed a novel mQβ-Globo-H conjugate (Scheme 1) by coupling Globo-H isothiocyanate (ITC) to the mQβ VLP. Importantly, the mQβ-Globo-H conjugate elicited robust Globo-H-specific IgG responses in both mice and rabbits. This study presents the first candidate for a Globo-H-VLP conjugate vaccine.



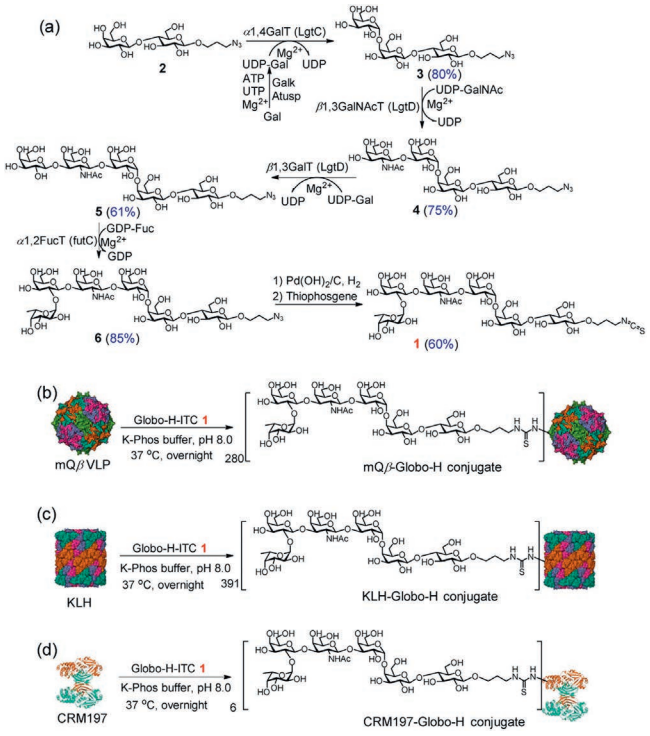
Scheme 1. A schematic diagram of the proposed mQβ-Globo-H conjugate designed to elicit robust anticancer IgG responses. The structure of mQβ (PDB ID: 7TJG) was sourced from the Protein Data Bank (PDB).

The pET28a-mQβ(A38K/A40C/D102C) recombinant plasmid, which encodes the coat protein, was constructed and transformed into BL21 (DE3) competent cells. The expression of the mQβ VLP was achieved through induction with isopropyl β-D-1-thiogalactopyranoside (IPTG). Following induction, the bacteria were sonicated to release the mQβ VLP. High-purity mQβ VLP was then obtained through a series of purification steps, including PEG8000 precipitation, *n*-butanol/chloroform extraction, and sucrose gradient centrifugation. The characterization of the purified mQβ VLPs was performed using several techniques: sodium dodecyl sulfate-polyacrylamide gel electrophoresis (SDS-PAGE), matrix-assisted laser desorption/ionization time-of-flight (MALDI-TOF) mass spectrometry (MS), transmission electron microscopy (TEM), and dynamic light scattering (DLS). Gel electrophoresis indicated that the mQβ VLP displayed a single band around 14 kDa (Fig. S1 in Supporting information). The MS result revealed a molecular weight of 14.2 kDa for the mQβ subunit (Fig. S2 in Supporting information). The TEM analysis revealed an average particle size of 28 nm for the mQβ VLP, as determined with nanomeasuring software, aligning with the DLS result (Fig. S3 in Supporting information). These results confirm that we have successfully prepared mQβ VLPs, consistent with previously reported work [24].

The synthesis of Globo-H-ITC **1** was accomplished using a chemoenzymatic method. Prior to the synthesis, we prepared the enzymes involved, which included *Neisseria meningitidis* α1,4-galactosyltransferase (LgtC) [29], *Escherichia coli* K-12 galactokinase (Galk), *Arabidopsis* UDP-sugar pyrophosphorylase (Atusp), the bifunctional β1,3-*N*-acetylgalactosaminyltransferase/β1,3-galactosyltransferase from *Haemophilus influenzae* (LgtD) [30], and *Helicobacter pylori* α1,2-fucosyltransferase (futC) (see Fig. S4 and the other Supporting information for further details) [31].

The chemoenzymatic synthesis of Globo-H-ITC **1** began with Lacβ-ProN_3 **2**. We added LgtC, Galk, and Atusp to a Tris–HCl buffer (100 mmol/L, pH 7.5) containing Gal, ATP, UTP, $MgCl_2$ and **2**, yielding Gb3-ProN_3 **3** with an 80% yield. Then, **3** was incubated with LgtD in the presence of UDP-GalNAc and $MgCl_2$, resulting in Gb4-ProN_3 **4**, achieved with a yield of 75%. Next, **4** was subjected to LgtD, UDP-Gal, and $MgCl_2$ in a Tris–HCl buffer (100 mmol/L, pH 7.5), producing Gb5-ProN_3 **5** with a yield of 61%. Following this, Globo-H-ProN_3 **6** was synthesized with an 85% yield by incubating Gb5-ProN_3 **5** with futC, GDP-Fuc and $MgCl_2$ in Tris–HCl (100 mmol/L, pH 7.5). Finally, the azido group of **6** was reduced through catalytic hydrogenolysis, yielding the Globo-H amine, which was reacted with thiophosgene to give the final product, Globo-H-ITC **1** (Scheme 2a). The final product and intermediates were characterized using proton (^{1}H) nuclear magnetic resonance spectroscopy (NMR), ^{13}C NMR, ^{1}H–^{1}H correlation spectroscopy (COSY), heteronuclear single quantum coherence (HSQC), heteronuclear multiple bond correlation (HMBC), and high-resolution mass spectrometry (HRMS) (see Supporting information for the characterization spectra).

Our chemoenzymatic synthesis of Globo-H offers a more efficient and streamlined approach compared to conventional methods. Starting with compound **2**, we established an optimized enzymatic cascade (LgtC/Galk/Atusp → LgtD → LgtD → futC), which avoids the need for intricate protecting group manipulations while maintaining high stereoselectivity and yield. Additionally, the final conversion from azido to ITC improves its applicability for bioconjugation. When compared to traditional chemical synthesis [32] and previous enzymatic routes [33], our method demonstrates greater efficiency, cost-effectiveness, and product purity, making it particularly suitable for the large-scale production of Globo-H-ITC for vaccine development.



Scheme 2. Syntheses of (a) Globo-H-ITC **1**, (b) mQβ-Globo-H, (c) KLH-Globo-H, and (d) CRM197-Globo-H conjugates. The structures of mQβ (PDB ID: 7TJG), KLH (PDB ID: 4BED), and CRM197 (PDB ID: 4AE0) were sourced from the PDB.

After acquiring mQβ VLP and Globo-H-ITC **1**, we proceeded to synthesize the mQβ-Globo-H conjugate. This was achieved by incubating Globo-H-ITC **1** with mQβ VLP in K-Phos buffer (0.1 mol/L, pH 8.0) overnight at 37 °C (Scheme 2b), the resulting mQβ-Globo-H conjugate was analyzed using MALDI-TOF, which revealed an average of 280 Globo-H molecules per mQβ VLP (Fig. S5 in Supporting information). As a control, we also created a KLH-Globo-H conjugate, in which Globo-H was conjugated to the KLH protein (Scheme 2c), resulting in an average of 391 Globo-H molecules per KLH molecule (Fig. S6 in Supporting information). Additionally, to compare our results with those from another classical vaccine carrier, we synthesized a CRM197-Globo-H conjugate (Scheme 2d), which contained an average of 6 Globo-H molecules per CRM197 molecule (Fig. S7 in Supporting Information).

After synthesizing and characterizing the conjugates, we assessed their immune properties in C57BL/6J female mice aged 6−10 weeks. The animal experiments were performed in accordance with the guidelines of the Animal Care and Use Committee of Shandong University and approved by the Animal Ethics Committee of the College of Life Sciences at Shandong University (No. SYDWLL-2023–044). On days 0, 14, and 28, six groups of C57BL/6J mice received subcutaneous immunization at the scruff of the neck with one of the following: mQβ, an admixture of mQβ + Globo-H, the mQβ-Globo-H conjugate, the CRM197-Globo-H conjugate, the KLH-Globo-H conjugate (which contained 6 μg of Globo-H per injection), and KLH alone (Fig. 1a). All immunizations were administered with MPLA [34] as an adjuvant. Sera were collected for enzyme-linked immunosorbent assay (ELISA) at pre-immunization (day −1) and post-immunization (days 7, 21, 35, 49, and 100). Additionally, Globo-H-ITC **1** was conjugated to bovine serum albumin (BSA) to create the BSA-Globo-H conjugate (Fig. S8 in Supporting information) for ELISA analysis of anti-Globo-H antibodies, thereby preventing interference from anti-mQβ antibodies.

As shown in Fig. 1b, the mean IgG titers produced by various groups in mice on day 35 were as follows: mQβ only (1452), the

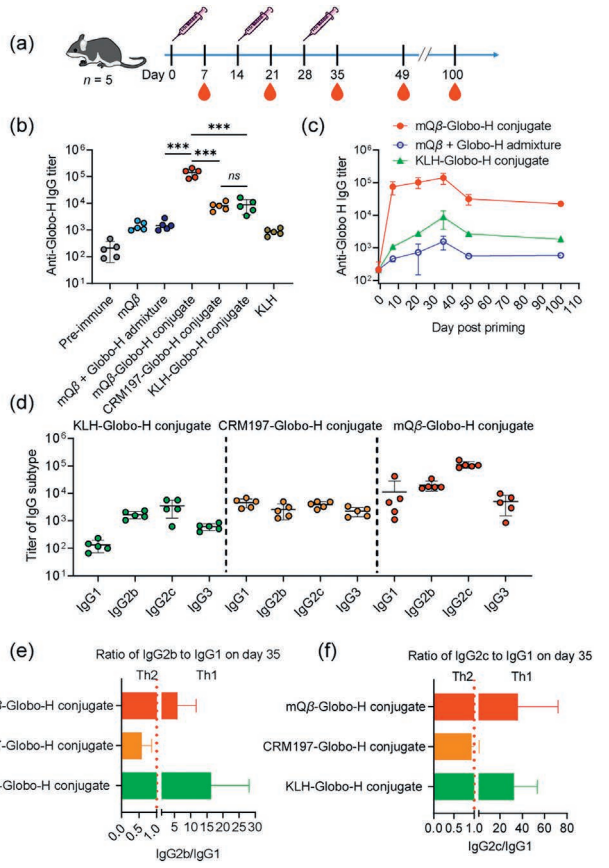


Fig. 1. Immunization of mice with the mQβ-Globo-H conjugate elicited a robust and long-lasting anti-Globo-H IgG response. (a) The timeline for mouse immunization and serum collection is illustrated. (b) The titers of anti-Globo-H antibodies were measured for various groups: mQβ, mQβ + Globo-H admixture, mQβ-Globo-H conjugate, CRM197-Globo-H conjugate, KLH-Globo-H conjugate, and KLH, all tested in mice. (c) The persistence of IgG responses induced by the mQβ-Globo-H conjugate is shown. (d) The IgG subtypes present in sera from mice immunized with the conjugates are displayed. (e) The ratios of IgG2b to IgG1 on day 35 are presented. (f) The ratios of IgG2c to IgG1 on day 35 are also provided. To detect anti-Globo-H IgG, the BSA-Globo-H conjugate was coated on a plate for ELISA measurements. Each symbol represents serum from an individual mouse. Data are presented as the mean ± standard deviation (SD) ($n = 5$). An unpaired two-tailed t-test using GraphPad Prism was employed to determine P-values. $^{***}P < 0.001$, ns: not significant.

admixture of mQβ + Globo-H (1577), the CRM197-Globo-H conjugate (8059), the KLH-Globo-H conjugate (8822), and KLH (867). In contrast, the mQβ-Globo-H conjugate elicited a mean anti-Globo-H IgG titer of 141,945, which is 16-fold higher than the mean titer of the KLH-Globo-H conjugate and 18-fold higher than that of the CRM197-Globo-H conjugate (Fig. 1b). The significantly higher anti-Globo-H IgG titers induced by the mQβ-Globo-H conjugate (*vs.* mQβ + Globo-H admixture) demonstrate that covalent conjugation to the mQβ carrier is critical for eliciting potent antibody responses. Additionally, the mQβ-Globo-H conjugate induced a durable anti-Globo-H IgG response, with a mean IgG titer of 22,445 on day 100, compared to an average IgG titer of only 1860 induced by the KLH-Globo-H conjugate on the same day (Fig. 1c).

IgG subtype analysis revealed that the mQβ-Globo-H conjugate induced higher titers of anti-Globo-H IgG1, IgG2b, IgG2c, and IgG3 compared to the KLH-Globo-H and CRM197-Globo-H conjugates. Among these, IgG2c was the predominant subtype for both the mQβ-Globo-H and KLH-Globo-H conjugates, whereas IgG1 dominated in the CRM197-Globo-H conjugate (Fig. 1d). The IgG2b/IgG1 and IgG2c/IgG1 ratios serve as indicators for Th1/Th2 bias: a ratio >1 indicates a Th1-skewed response, a ratio =1 suggests a balanced Th1/Th2 response, and a ratio <1 reflects a Th2-skewed re-

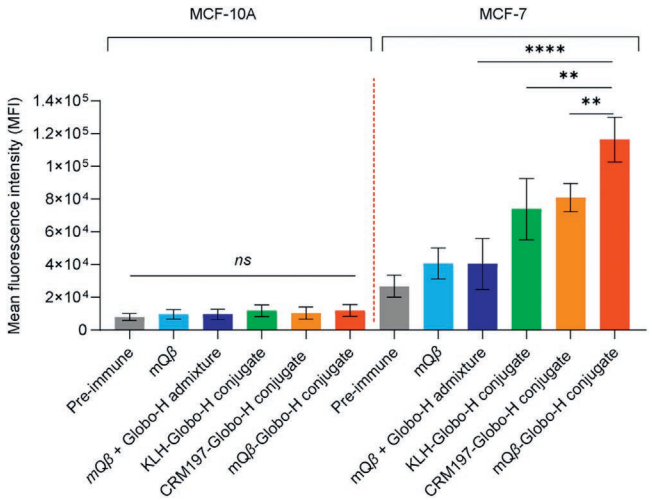


Fig. 2. Analysis using FACS revealed that IgG antibodies induced by the mQβ-Globo-H conjugate bound strongly to MCF-7 cancer cells, while exhibiting no binding to normal MCF-10A cells. The assay was conducted using a 1:20 dilution of serum with five mice per group. Data are presented as the mean ± SD ($n = 5$). An unpaired two-tailed *t*-test was performed using GraphPad Prism to determine *P*-values. $^{**}P < 0.01$, $^{****}P < 0.0001$.

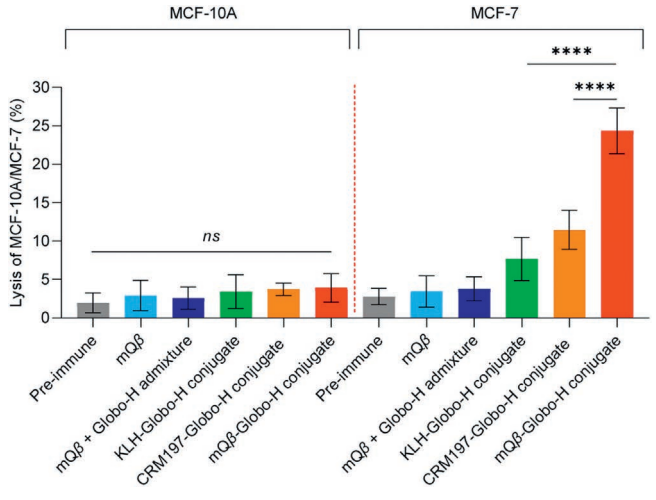


Fig. 3. Sera from the mQβ-Globo-H conjugate exhibited significantly higher CDC towards MCF-7 cells compared to sera from the mQβ + Globo-H admixture, KLH-Globo-H conjugate, and CRM197-Globo-H conjugate ($n = 5$ mice per group). Data are presented as the mean ± SD ($n = 5$). An unpaired two-tailed *t*-test was conducted using GraphPad Prism to determine the *P*-value. $^{****}P < 0.0001$.

sponse [35,36]. As shown in Figs. 1e and f, both the mQβ-Globo-H and KLH-Globo-H conjugates skewed the immune response toward Th1, whereas the CRM197-Globo-H conjugate favored a Th2 response. Notably, the stronger Th1-weighted immune response induced by the mQβ-Globo-H conjugate is likely attributable to the encapsulation of single-stranded RNAs derived from *E. coli* within the mQβ VLP. These RNAs serve as effective agonists for Toll-like receptors 7 (TLR7) and 8 (TLR8), thereby enhancing immune responses and promoting a Th1 bias [21,37].

The capability of serum antibodies to recognize antigens on cell surfaces was assessed using fluorescence-activated cell sorting (FACS). MCF-7 human breast cancer cells and MCF-10A human mammary epithelial cells were used for this analysis. The procedure involved incubating the cells with serum in FACS buffer for 30 min on ice. After incubation, the cells were washed with FACS buffer and further incubated with a fluorescein isothiocyanate (FITC)-labeled goat anti-mouse IgG antibody for another 30 min. Following another wash with FACS buffer, the cells were analyzed *via* flow cytometry. As shown in Fig. 2, antibodies generated by the mQβ-Globo-H conjugate demonstrated strong binding to Globo-H-positive MCF-7 cancer cells. In contrast, antibodies produced from an admixture of mQβ + Globo-H exhibited weak binding to MCF-7 cells. This observation emphasizes the importance of the covalent conjugation of Globo-H to mQβ. Furthermore, the binding strength of antibodies derived from the mQβ-Globo-H conjugate was significantly greater than that of antibodies induced by the CRM197-Globo-H and KLH-Globo-H conjugates (Fig. 2), suggesting that the mQβ-Globo-H conjugate serves as a superior anticancer vaccine. Additionally, antibodies produced by the mQβ-Globo-H conjugate did not bind to MCF-10A cells (Fig. 2), indicating that these antibodies do not recognize normal breast cells. This specificity underscores their safety for potential therapeutic use.

Serum antibody-mediated cell killing is assessed through CDC. MCF-7 cells were incubated with post-immunization sera from various mouse groups: Those immunized with mQβ, an admixture of mQβ + Globo-H, the mQβ-Globo-H conjugate, the KLH-Globo-H conjugate, and the CRM197-Globo-H conjugate. Rabbit complement was then added to the serum-incubated cells, and the MTS assay was employed to measure CDC-induced killing. As shown in Fig. 3, the antibody-mediated killing of MCF-7 cell induced by the mQβ-Globo-H conjugate was significantly greater than that triggered by sera from mice immunized with the KLH-Globo-H conjugate or the CRM197-Globo-H conjugate when complement was present. Importantly, the antibodies generated by the mQβ-Globo-H conjugate did not result in any significant killing of MCF-10A normal cells above background. These results suggest that the mQβ-Globo-H conjugate elicits a robust IgG response against Globo-H, specifically targeting and killing Globo-H-positive cancer cells.

To advance clinical translation and further evaluate the humoral immunity of the mQβ-Globo-H conjugate, rabbits were immunized with either free mQβ or the mQβ-Globo-H conjugate on days 0, 14, and 28, using complete Freund's adjuvant (CFA) and incomplete Freund's adjuvant (IFA) as adjuvants (Fig. 4a). Pre- and post-immunization sera were collected for immunological evaluation experiments, including ELISA, and CDC. As shown in Fig. 4b, immunizing rabbits with the mQβ-Globo-H conjugate resulted in a high anti-Globo-H IgG titer of 1604,140 by day 35. In contrast, vaccination with mQβ alone generated only an average IgG titer of 1600. The CDC killing of MCF-7 cells by rabbit sera, assessed before and after immunization with either mQβ or mQβ-Globo-H conjugate, was 1.6 %, 4 %, and 30.1 %, respectively (Fig. 4c). These results indicate a significant CDC killing effect of the rabbit antibodies elicited by the mQβ-Globo-H conjugate on MCF-7 cells. Furthermore, sera from rabbits immunized with the mQβ-Globo-H conjugate showed no killing effect on normal MCF-10A cells compared to the background (Fig. 4c). Overall, these findings suggest that the mQβ-Globo-H conjugate can produce potent, Globo-H-specific IgG antibodies in rabbits.

To evaluate the translational potential of the mQβ-Globo-H conjugate vaccine in human patients, we procured a microarray of human triple-negative breast cancer tissues (HBreD180Bc01–1). The tissues were stained using a 1:500 dilution of serum from a rabbit that had been immunized with the mQβ-Globo-H conjugate. The results indicated that 146 out of 150 cancer samples showed positive binding to the mQβ-Globo-H postimmunization serum (97 % positive staining, Fig. S9 in Supporting information). In comparison, a second human breast cancer tissue microarray (HBreD055CD01) from 55 different patients was stained with serum from rabbits immunized with mQβ only. The staining observed in all these cancer tissues was negligible (Fig. S10 in Supporting information). These results demonstrate that Globo-

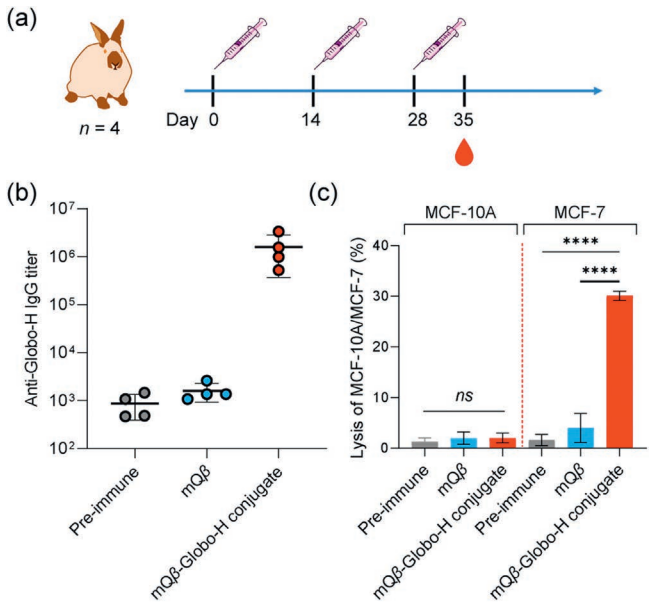


Fig. 4. Immunization of rabbits with the mQβ-Globo-H conjugate induced a robust anti-Globo-H IgG response. (a) Rabbit immunization is depicted. (b) Titers of anti-Globo-H IgG antibodies elicited by the mQβ-Globo-H conjugate in rabbits. Each symbol represents the serum from an individual rabbit. (c) Sera from the rabbits immunized with the mQβ-Globo-H conjugate displayed high CDC against MCF-7 cells ($n = 4$ rabbits per group). Data are presented as the mean ± SD ($n = 4$). An unpaired two-tailed *t*-test conducted using GraphPad Prism was employed to calculate the *P*-value. $^{****}P < 0.0001$.

H-specific antibodies produced by the mQβ-Globo-H conjugate exhibit significant selectivity against human breast cancer tissues.

In conclusion, although significant efforts have been made to improve the immunogenicity of Globo-H (and its modified forms) by conjugating it with carriers such as KLH, CRM197, or MPLA, no Globo-H-based vaccine has yet succeeded clinically. This lack of success may stem from insufficient antibody quality and quantity generated by current approaches, which fail to confer broad tumor protection in patients. Thus, developing novel strategies for Globo-H conjugate design remains an urgent priority. In this study, we report the first successful covalent conjugation of chemoenzymatically synthesized Globo-H hexasaccharide to mQβ VLPs, creating the mQβ-Globo-H conjugate. Notably, this conjugate elicited substantially higher titers of anti-Globo-H IgG antibodies than both KLH-Globo-H and CRM197-Globo-H conjugates in comparative studies. The resulting antibodies exhibited specific binding to Globo-H-expressing cancer cells and demonstrated potent CDC against these target cells. Crucially, the antibodies by the mQβ-Globo-H conjugate showed exceptional tissue specificity for Globo-H-positive human breast cancer specimens, underscoring its clinical translational value. These collective findings establish the mQβ-Globo-H conjugate as a particularly promising platform for anticancer vaccine development. As the first reported VLP-based Globo-H conjugate vaccine, this work represents a meaningful breakthrough in carbohydrate-based cancer immunotherapy.

Declaration of competing interest

The authors declare that they have no known competing financial interests or personal relationships that could have appeared to influence the work reported in this paper.

CRediT authorship contribution statement

Yuanzhan Wang: Writing – original draft, Validation, Methodology, Formal analysis, Data curation. **Qingyu Zhao:** Methodology, Formal analysis. **Xuanjun Wu:** Writing – review & editing, Writing – original draft, Supervision, Resources, Project administration, Methodology, Funding acquisition, Conceptualization.

Acknowledgments

This work was financially supported by the Excellent Youth Fund Project supported by Shandong Provincial Natural Science Foundation (No. ZR2022YQ17), the Taishan Scholars Program for Young Experts of Shandong Province (No. tsqn202312047), and the National Natural Science Foundation of China (No. 22377065).

Supplementary materials

Supplementary material associated with this article can be found, in the online version, at doi:10.1016/j.cclet.2025.111642.

References

[1] R.D. Astronomo, D.R. Burton, Nat. Rev. Drug Discov. 9 (2010) 308–324.
[2] D. Li, H. Hong, H. Lin, et al., Chin. Chem. Lett. 37 (2026) 111324.
[3] H. Lin, Y. Li, K. Zhou, et al., Chin. Chem. Lett. 35 (2024) 108670.
[4] M.M. Wei, Y.S. Wang, X.S. Ye, Med. Res. Rev. 38 (2018) 1003–1026.
[5] S. Zhang, C. Cordon-Cardo, H.S. Zhang, et al., Int. J. Cancer 73 (1997) 42–49.
[6] G. Ragupathi, T.K. Park, S. Zhang, et al., Angew. Chem. Int. Ed. 36 (1997) 125–128.
[7] T. Gilewski, G. Ragupathi, S. Bhuta, et al., Proc. Natl. Acad. Sci. U. S. A. 98 (2001) 3270–3275.
[8] C.S. Huang, A.L. Yu, L.M. Tseng, et al., J. Immunother. Cancer 8 (2020) e000342.
[9] H.S. Rugo, J. Cortes, B. Xu, et al., J. Clin. Oncol. 40 (2022) suppl.TPS611.
[10] Y.L. Huang, J.T. Hung, S.K.C. Cheung, et al., Proc. Natl. Acad. Sci. U. S. A. 110 (2013) 2517–2522.
[11] H.Y. Lee, C.Y. Chen, T.I. Tsai, et al., J. Am. Chem. Soc. 136 (2014) 16844–16853.
[12] C.Y. Chen, Y.W. Lin, S.W. Wang, et al., ACS Cent. Sci. 8 (2022) 77–85.
[13] C. Zhai, X.J. Zheng, C. Song, X.S. Ye, RSC Med. Chem. 12 (2021) 1239–1243.
[14] W. Ma, Z. Xu, C. Teng, et al., Angew. Chem. Int. Ed. 64 (2025) e202418948.
[15] Z. Zhou, G. Liao, S.S. Mandal, S. Suryawanshi, Z. Guo, Chem. Sci. 6 (2015) 7112–7121.
[16] S.J. Danishefsky, Y.K. Shue, M.N. Chang, C.H. Wong, Acc. Chem. Res. 48 (2015) 643–652.
[17] M.F. Bachmann, U.H. Rohrer, T.M. Kündig, et al., Science 262 (1993) 1448–1451.
[18] B. Akache, R.D. Weeratna, A. Deora, et al., Vaccines 4 (2016) 3.
[19] Z. Yin, M. Comellas-Aragones, S. Chowdhury, et al., ACS Chem. Biol. 8 (2013) 1253–1262.
[20] Z. Yin, S. Chowdhury, C. McKay, et al., ACS Chem. Biol. 10 (2015) 2364–2372.
[21] Z. Yin, S. Dulaney, C.S. McKay, et al., ChemBioChem 17 (2016) 174–180.
[22] X. Wu, Z. Yin, C. McKay, et al., J. Am. Chem. Soc. 140 (2018) 16596–16609.
[23] X. Wu, J. Ye, A.T. DeLaitsch, et al., Angew. Chem. Int. Ed. 60 (2021) 24179–24188.
[24] S. Sungsuwan, X. Wu, V. Shaw, et al., ACS Chem. Biol. 17 (2022) 3047–3058.
[25] Z. Rashidijahanabad, S. Ramadan, N.A. O'Brien, et al., Angew. Chem. Int. Ed. 62 (2023) e202309744.
[26] F. Shafieichaharberoud, S. Lang, C. Whalen, et al., Bioconjug. Chem. 35 (2024) 164–173.
[27] Z. Tan, C. Yang, P. Lin, et al., Adv. Healthc. Mater. 13 (2024) 2302755.
[28] Z. Tan, W. Yang, N.A. O'Brien, et al., Nat. Commun. 15 (2024) 3420.
[29] P. Zhu, C.M. Tsai, C.E. Frasch, FEMS Immunol. Med. Microbiol. 34 (2002) 193–200.
[30] J. Shao, J. Zhang, P. Kowal, Y. Lu, P.G. Wang, Biochem. Biophys. Res. Commun. 295 (2002) 1–8.
[31] D.B. Stein, Y.N. Lin, C.H. Lin, Adv. Synth. Catal. 350 (2008) 2313–2321.
[32] T.K. Park, I.J. Kim, S. Hu, et al., J. Am. Chem. Soc. 118 (1996) 11488–11500.
[33] D.M. Su, H. Eguchi, W. Yi, et al., Org. Lett. 10 (2008) 1009–1012.
[34] E. Vacchelli, L. Galluzzi, A. Eggermont, et al., Oncoimmunology 1 (2012) 894–907.
[35] O.A. Ortega-Rivera, M.D. Shin, A. Chen, et al., J. Am. Chem. Soc. 143 (2021) 14748–14765.
[36] V. Lensch, A. Gabba, R. Hincapie, et al., ACS Nano 18 (2024) 26770–26783.
[37] M.P. Schön, M. Schön, Oncogene 27 (2008) 190–199.